

# Differential Changes in the Cellular Composition of the Developing Marsupial Brain

Adele M.H. Seelke,<sup>1</sup> James C. Dooley,<sup>1</sup> and Leah A. Krubitzer<sup>1,2\*</sup>

<sup>1</sup>Center for Neuroscience, University of California, Davis, Davis, California 95618

<sup>2</sup>Department of Psychology, University of California, Davis, Davis, California 95618

## ABSTRACT

Throughout development both the body and the brain change at remarkable rates. Specifically, the number of cells in the brain undergoes dramatic nonlinear changes, first exponentially increasing in cell number and then decreasing in cell number. Different cell types, such as neurons and glia, undergo these changes at different stages of development. The current investigation used the isotropic fractionator method to examine the changes in cellular composition at multiple developmental milestones in the short-tailed opossum, *Monodelphis domestica*. Here we report several novel findings concerning marsupial brain development and organization. First, during the later stages of neurogenesis (P18), neurons make up most of the cells in the neocortex, although the total number of neurons remains the same throughout the life span. In contrast, in the subcortical

regions, the number of neurons decreases dramatically after P18, and a converse relationship is observed for nonneuronal cells. In the cerebellum, the total number of cells gradually increases until P180 and then remains constant, and then the number of neurons is consistent across the developmental ages examined. For the three major structures examined, neuronal density and the percentage of neurons within a structure are highest during neurogenesis and then decrease after this point. Finally, the total number of neurons in the opossum brain is relatively low compared with other small-brained mammals such as mice. The relatively low number of neurons and correspondingly high number of nonneurons suggests that in the marsupial brain nonneurons may play a significant role in signal processing. *J. Comp. Neurol.* 521:2602–2620, 2013.

© 2013 Wiley Periodicals, Inc.

**INDEXING TERMS:** development; marsupials; neocortex; evolution; comparative neuroanatomy; isotropic fractionation

Throughout development, both the body and the brain undergo remarkable changes in both size and function. Because the nature of brain–body relationships and the cellular composition and state of connectivity of the brain itself are fundamentally different at various stages of development, it is important to consider each developmental stage in its own right rather than as a continuum of the same structure that changes from simple to complex. This is particularly true because some cells play radically different roles at different stages of development (Polazzi and Contestabile, 2002). Traditionally, when we consider brain development, we focus on neural development: how neurons are generated; how they migrate; and ultimately how they differentiate, connect, and refine their structure. The importance of neural development is undeniable, but the brain is not composed of neurons alone. Other cell types, including but not limited to endothelial cells (capillaries and blood vessels), mesothelial cells (pia mater), ependymal cells (lining of the ventricles), and glial cells, are present as well, and, among these, glia are the most prevalent (Morest

and Silver, 2003; Temple, 2001). Recent studies have underscored the importance of microglia cells in both neurogenesis (Cunningham et al., 2012) and programmed cell death (Kriegstein and Noctor, 2004; Polazzi and Contestabile, 2002; Uponder and Naegele, 1999) and of astrocytes in synaptic transmission and plasticity in adults (Nadarajah and Parnavelas, 2002; Rakic, 1990; Santello et al., 2012).

The current study examines the developmental relationships between neuronal and nonneuronal cells in the brains of short-tailed opossums using the isotropic fractionator technique. This relatively new methodology allows one to estimate quickly and reliably the number of neuronal and nonneuronal cells in different structures of the brain (Herculano-Houzel and Lent, 2005). This is

Grant sponsor: National Institutes of Health; Grant number: R21NS071225 (to L.A.K.); Grant number: T32EY015387 (to J.C.D.).

\*CORRESPONDENCE TO: Leah A. Krubitzer, Center for Neuroscience, 1544 Newton Ct., Davis, CA 95616. E-mail: lakrubitzer@ucdavis.edu

Received August 11, 2012; Revised September 18, 2012; Accepted January 4, 2013

DOI 10.1002/cne.23301

Published online January 16, 2013 in Wiley Online Library (wileyonlinelibrary.com)

© 2013 Wiley Periodicals, Inc.

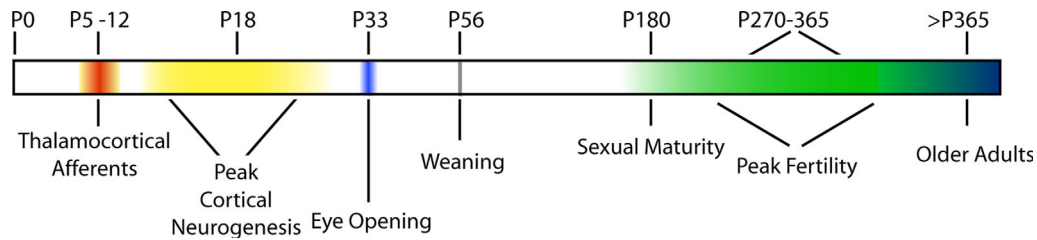


**Figure 1.** Timeline of significant postnatal developmental milestones in the life of *Monodelphis domestica*. Thalamocortical connections are formed between P5 and P12 (red). Peak cortical neurogenesis occurs from P14 to P24 (yellow). Eyes open between P31 and P34 (blue). Opossums are separated from their mothers at P56 (gray) and reach sexual maturity by P180 (green). Their peak reproductive period is from P270 to P365, and after P365 they enter old age.

**TABLE 1.**  
Age, Sex, and Weight of Animals

Case No.	Group	Weight (g)	Sex
12-060	P18	3	f
12-061	P18	3	m
12-062	P18	2	m
12-064	P18	2	f
11-148	P35	7	f
11-149	P35	9	f
11-235	P35	7	f
11-236	P35	5	f
11-237	P35	7	m
11-157	P56	13	f
11-158	P56	13	f
11-160	P56	15	f
11-240	P56	13	m
11-241	P56	13	m
11-150	P180	77	m
11-159	P180	96	f
11-162	P180	59	f
11-267	P180	99	m
11-268	P180	131	m
11-154	P270-365	75	f
11-156	P270-365	137	m
11-161	P270-365	64	f
11-242	P270-365	86	f
11-151	>P365	148	m
11-152	>P365	121	f
11-153	>P365	107	f
11-155	>P365	134	m
11-243	>P365	109	m

accomplished by transforming anisotropic structures of the brain, such as the six-layered neocortex, into an isotropic suspension of cell nuclei. These nuclei can be labeled using immunohistochemical techniques that identify them as neurons or other types of cells. The nuclei are then counted, and the total number of cells, as well as the number of neuronal and nonneuronal cells, can be calculated. Because these techniques are independent of total brain volume, they are ideal for a number of important

developmental comparisons across different age groups in which overall brain volume changes dramatically.

We used short-tailed opossums, because they are born in a very immature state, the equivalent to embryonic day (E) 13–14 in rats (Saunders et al., 1989). Furthermore, infant opossums are not housed within a pouch, so they are easily accessible for manipulation and tissue harvest. Finally, compared with placental (eutherian) mammals such as rodents, the significant events of brain and sensory development occur over a protracted period, extending past the first postnatal month (Fig. 1; Saunders et al., 1989). Thus, the short-tailed opossum is an excellent model for studying both early brain development and adult cortical composition.

The goal of the present investigation was to examine the neuronal and nonneuronal composition of different structures of the developing brain, including the neocortex, cerebellum, and subcortical structures across important developmental time points. We found that, whereas the total number of cells increases across development, the proportion of neurons generally decreases across development, and the cellular composition of different regions of the brain follows distinct and different developmental trajectories. These findings represent the first quantification of the cellular composition of a marsupial brain across several important developmental stages.

## MATERIALS AND METHODS

The isotropic fractionation procedure consists of multiple stages. First, tissue was dissected into major structures. Next, tissue was processed, which included homogenization, DAPI staining, and NeuN immunohistochemistry. The third stage involved quantifying the number of DAPI-labeled nuclei within a sample, and the fourth stage involved determining the proportion of NeuN-labeled nuclei within that same sample. Finally, in the last stage, we used these values to calculate the total number of cells, total number of neurons, total number of nonneurons, cell

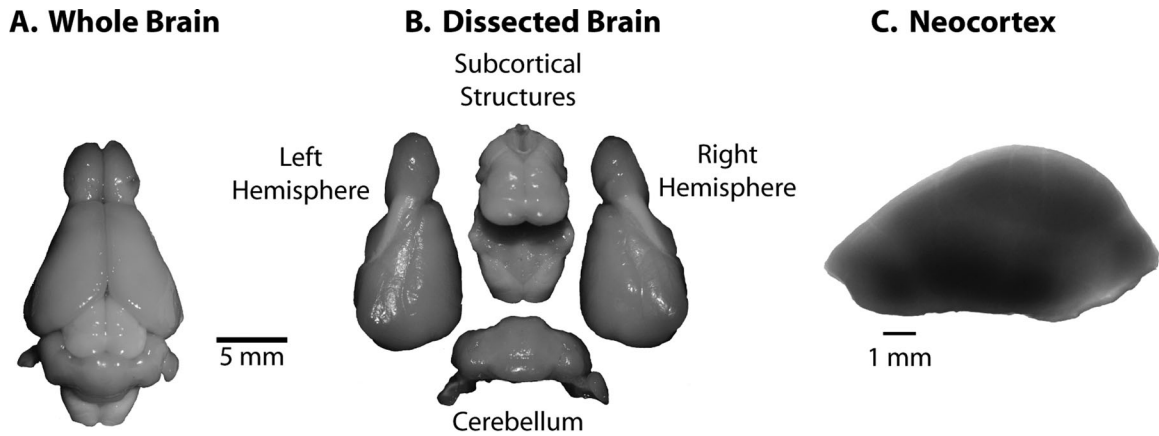


**Figure 2.** Dissection of the brain for isotropic fractionation. The whole brain (A) is separated into the left and right cerebral hemispheres, subcortical structures (including the midbrain, thalamus, hypothalamus, and brainstem), and cerebellum (B). The cerebral hemispheres are further dissected, removing the olfactory bulb, pyriform cortex, basal ganglia, and hippocampus, until only the neocortex remains (C). Scale bars = 5 mm in A,B; 1 mm in C.

density, neuronal density, and nonneuronal density. Each of these stages is discussed in detail below.

## Subjects

Thirty South American short-tailed opossums (*Mondelphis domestica*) raised in our breeding colony at the University of California, Davis, were used in these experiments. Opossums were examined at six developmentally significant ages: during cortical neurogenesis (P18, N = 4), eye opening (P35 ± 1 day, N = 5), weaning (P56 ± 1 day, N = 5), sexual maturity (P180 ± 1 day, N = 5), adulthood (P270–365, N = 4), and elderly adulthood (>P365, N = 5; see Table 1 for sexes and weights). Two additional animals, one at P18 and one at P180, were used to show the relationship between neurons and non-neurons in nonhomogenized tissue. All experiments were performed under National Institutes of Health guidelines for the care of animals in research and were approved by the Institutional Animal Care and Use Committee of the University of California, Davis.

## Tissue dissection

Animals were euthanized with an overdose of sodium pentobarbital (Beuthanasia; 250 mg/kg) and transcardially perfused with phosphate-buffered saline, followed by 4% paraformaldehyde. The brain was extracted, photographed, and weighed. Under a microscope, the brain was dissected into sections: the left cortical hemisphere, right cortical hemisphere, cerebellum, and remaining subcortical regions (including the hypothalamus, thalamus, and brainstem; Fig. 2). The neocortex was then isolated by removing the hippocampus, basal ganglia, pyriform cortex, and olfactory bulb from the cortical hemisphere.

These sections were photographed and weighed, then placed in 5% paraformaldehyde for storage.

## Tissue processing

Tissue was homogenized in a 15-ml glass Kontes Tenbroek tissue grinder (Kimble Chase) with a dissociation solution composed of 10 ml Triton X-100 and 11.76 g sodium citrate in 1,000 ml distilled water. The homogenization process broke down cell membranes, producing a suspension of isolated cellular nuclei with no visible tissue clumps. An aliquot from the main suspension was centrifuged and resuspended in a solution of phosphate-buffered saline (PBS) and 4',6-diamidino-2-phenylindole (DAPI), which binds to DNA and labels all cellular nuclei regardless of cell type (Fig. 3A,D,G). If the tissue had been stored in fixative for more than 4 weeks, the sample was suspended in a boric acid solution (12.37 g in 1,000 ml distilled water) and placed in an oven at 70°C for 1 hour for epitope retrieval. A separate aliquot from the main suspension was stained for neuronal nuclei using immunocytochemical techniques with the anti-NeuN antibody (Millipore, Bedford, MA; see Table 2 for antibody description). Alexa Fluor 647 or Alexa Fluor 700 goat anti-mouse IgG secondary antibody (Invitrogen, Carlsbad, CA) was used to fluorescently tag NeuN-labeled nuclei (Fig. 3B,E,H). In selected cases, we also used Alexa Fluor 594 goat anti-mouse IgG secondary antibody (Invitrogen) to tag NeuN-labeled nuclei fluorescently.

## Antibody characterization

See Table 2 for a list of the antibodies used. NeuN antibody (clone A60) specifically recognizes the DNA-binding, neuron-specific protein NeuN, which is present in most

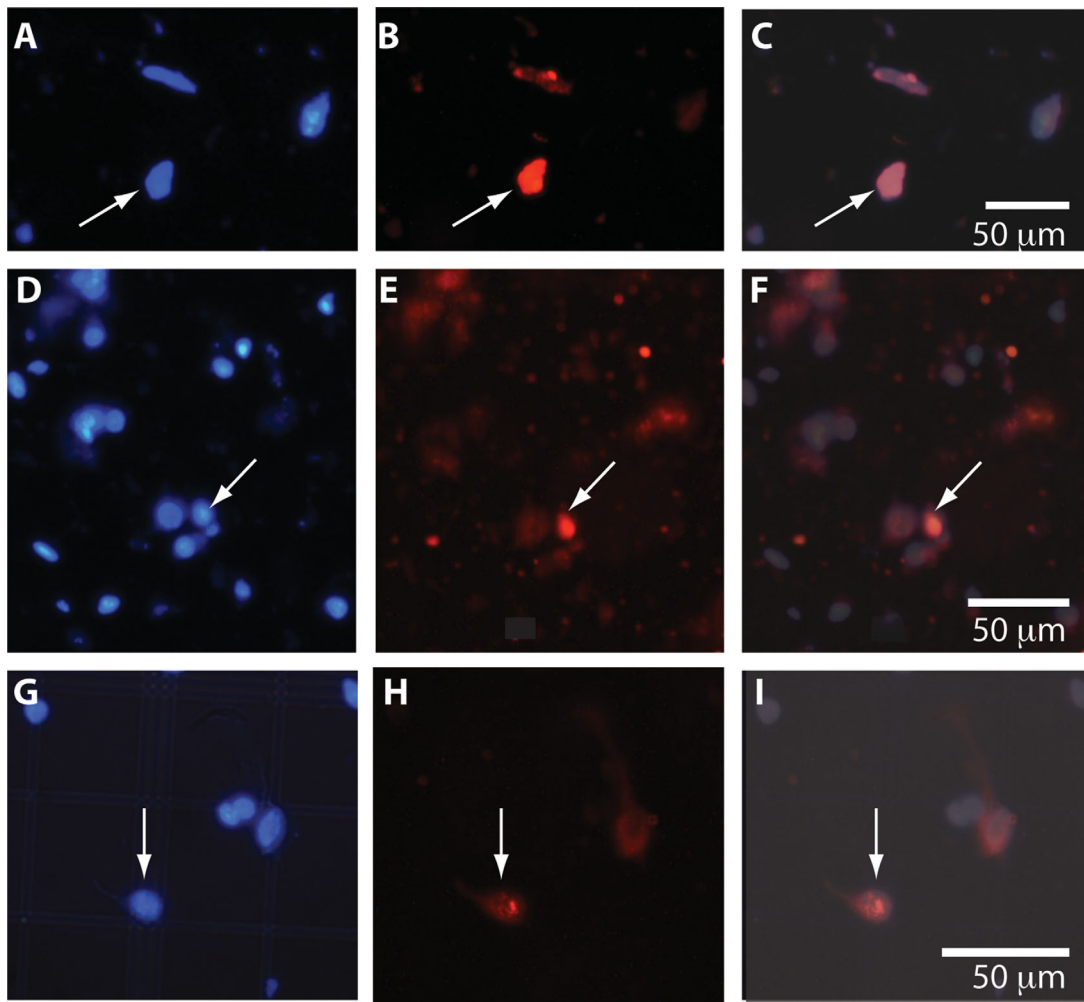


**Figure 3.** Distribution of DAPI<sup>+</sup> and NeuN<sup>+</sup> nuclei following tissue dissociation. Cellular nuclei from the neocortex (top row), subcortical regions (middle row), and cerebellum (bottom row) were dissociated and stained for DAPI (labeled in blue; A,D,G) and NeuN (labeled in red; B,E,H). Nuclei that are stained for both DAPI and NeuN are considered to be neuronal (labeled in pink; C,F,I). Arrows identify one nucleus in each brain region that is both DAPI<sup>+</sup> and NeuN<sup>+</sup>. Color and contrast have been adjusted in Adobe Photoshop. Scale bars = 50  $\mu$ m.

**TABLE 2.**  
Antibody Used

Antigen	Immunogen	Manufacturer, species, mono- vs. polyclonal, catalog No.	Dilution used
NeuN	Purified cell nuclei from mouse brain	Millipore (Billerica, MA), mouse monoclonal, MAB377	1:300

central and peripheral nervous system neuronal cell types of all vertebrates tested. However, there are some exceptions that are described in the Discussion. In a Western blot analysis, this antibody recognized two or three bands in the 46–48 kDa range and possibly another band at approximately 66 kDa (adapted from product information). Because NeuN specifically stains neuronal nuclei, staining of nonneuronal tissue was used as a negative control.

### Nuclei quantification

The total number of nuclei was determined using a Neubauer cell-counting chamber (Optik Labor). Samples were vortexed, and 10  $\mu$ l aliquots were immediately loaded into a Neubauer cell-counting chamber and placed on a fluorescence microscope for visualization and counting of nuclei. Standard stereological protocols were used (Mouton, 2002). To obtain a reliable and representative sample of the number of DAPI-labeled nuclei within a

given sample size, we counted the nuclei in one 8-square by 8-square section of the Neubauer chamber (for details see Campi et al., 2011). We repeated these counts on multiple samples until we had counted 10 unique  $8 \times 8$  sections. We then calculated the mean number of nuclei in an  $8 \times 8$  section and used that number to determine the total number of nuclei in the sample, using the equation described below.

### Determining NeuN<sup>+</sup> percentage

With a separate aliquot from the main suspension, the ratio of neuronal to nonneuronal nuclei within a sample was determined using a flow cytometer at the UC Davis Flow Cytometry Shared Resource Center. The use of a flow cytometer to automate the detection and counting of neuronal and nonneuronal nuclei is both faster and more reliable than visual inspection under a fluorescent microscope (Collins et al., 2010b). To quantify the proportion of neuronal nuclei, we used a Becton Dickinson (BD) Five-Laser LSRII flow cytometer. The violet laser (50 mW, 405 nm) excites DAPI-labeled nuclei, and the red laser (50 mW, 635 nm) excites both Alexa Fluor (AF) 647-labeled nuclei and AF 700-labeled nuclei. For all samples, between 1,000 and 10,000 DAPI-positive nuclei were evaluated for AF 647 and AF 700 label. Samples run on the flow cytometer were forced through a 35- $\mu$ m mesh cell filter, vortexed, and immediately taken into the LSRII. Selection gates were determined by a flow cytometry expert who was blind to the developmental stage and brain areas of the samples. The selection gates used to estimate NeuN-IR nuclei were constructed to minimize the amount of both myelin debris and clumps of nuclei (i.e., doublets and triplets) that were counted within the samples. The samples were run for 120 seconds or until 10,000 nuclei had been detected. The ratio of neuronal to nonneuronal nuclei was estimated from the gated population (see equations below).

To ensure the reliability of our results, in several cases we reanalyzed samples of dissociated and stained tissue. We did not see any significant differences between the first and second sets of analyses. Additionally, as mentioned above, in selected cases we labeled neuronal nuclei with AF 594 and counterstained them with DAPI. This allowed us to perform manual counts of NeuN<sup>+</sup> and DAPI<sup>+</sup> nuclei on a fluorescent microscope. The UV filter excited the DAPI-labeled nuclei, and the TRITC filter excited the AF 594-labeled nuclei. We used a Neubauer cell counting chamber to count the number of DAPI-labeled and AF 594-labeled nuclei. We then calculated the proportion of NeuN<sup>+</sup> to DAPI<sup>+</sup> nuclei and compared that with the results obtained using the flow cytometer. We did not see any significant differences between these sets of analyses.

### Equations

Estimates of cellular composition for a given structure were derived from the following equations.

$$\begin{aligned} \text{Total nuclei} &= [(\text{number of DAPI}^+ \text{ nuclei}) \\ &/(\text{volume of suspension counted in mm}^3)] \\ &\times (\text{total suspension volume in cm}^3) \times 1,000 \end{aligned}$$

$$\text{Percentage neurons} = (\text{number of NeuN}^+ \text{ nuclei}) / (\text{number of DAPI}^+ \text{ nuclei})$$

$$\text{Total neurons} = \text{percent neurons} \times \text{total nuclei}$$

$$\text{Total nonneurons} = \text{total nuclei} - \text{total neurons}$$

$$\text{Cell density} = \text{number of cells} / \text{weight of structure}$$

$$\text{Neuron density} = \text{number of neurons} / \text{weight of structure}$$

$$\text{Nonneuron density} = \text{number of nonneurons} / \text{weight of structure}$$

### Analysis

Developmental changes in the weights of the whole brain, neocortex, subcortical structures, cerebellum, and brain weight to body weight ratio were assessed by ANOVA (JMP; SAS, Cary, NC), and differences between specific age groups were determined using Student's *t*-tests. Likewise, developmental differences in the percentage of neurons, total number of cells, total number of neurons, total number of nonneurons, cell density, neuronal density, and nonneuronal density were assessed by ANOVA, and differences between specific age groups were determined by using Student's *t*-tests. For all tests,  $\alpha = 0.05$ .

### Whole-section staining

In two additional cases, we show the relationship between DAPI- and NeuN-labeled cells in nonhomogenized tissue (Figs. 4–6). Each brain was sliced on a freezing microtome into 50- $\mu$ m horizontal sections. Briefly, the 50- $\mu$ m-thick free-floating sections were first rinsed ( $3 \times 5$  minutes) in PBS. To quench endogenous peroxidase, sections were incubated in an aqueous solution of 10% MeOH and 3% H<sub>2</sub>O<sub>2</sub> for 30 minutes at room temperature. After rinses in PBS-0.1% Triton X-100 ( $3 \times 10$  minutes), nonspecific binding was suppressed by a preincubation in 10% normal goat serum (NGS; Invitrogen) and PBS-0.1% Triton X-100 for 1 hour at room temperature. Sections were then transferred to the primary antibody solution (mouse anti-NeuN, 1:100; Millipore) containing 10% NGS and PBS-0.1% Triton X-100 overnight at 4°C. Tissue sections were then rinsed in PBS-0.1% Triton X-100 ( $4 \times 10$  minutes) and incubated in a secondary antibody solution (Cy3 goat anti-mouse IgG, 1:200; Millipore) for 4 hours at room temperature. The tissue sections were then

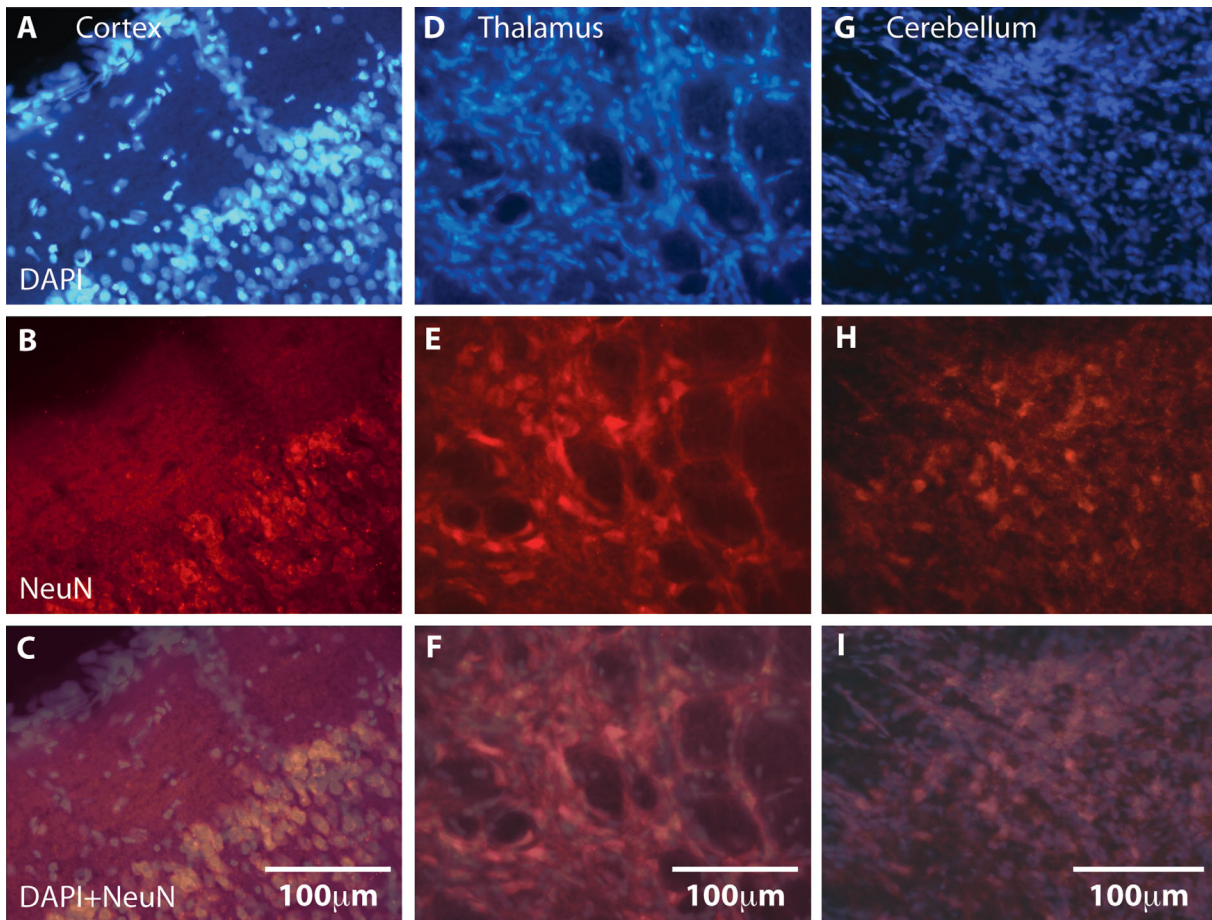


**Figure 4.** The normal, anisotropic distribution of DAPI<sup>+</sup> and NeuN<sup>+</sup> cells in portions of the neocortex (A–C), dorsal thalamus (D–F), and cerebellum (G–I) in a P180 brain. The superimposition of DAPI<sup>+</sup> (blue; A,D,G) and NeuN<sup>+</sup> (red; B,E,H) cells reveals the distribution of neurons (pink; C,F,I) relative to all cells. In this low-power image the densely packed neurons in cortical layers 2–3 are clearly evident (C). Neurons in this portion of the dorsal thalamus are more evenly distributed. The high-power images of the cerebellum (G–I) show that the number of neurons is relatively low (H) compared with the total numbers of cells (G,I). Color and contrast have been adjusted in Adobe Photoshop. Scale bars = 100  $\mu$ m.

thoroughly rinsed in PBS ( $3 \times 10$  minutes). The fluorescent sections were double-labeled with the nuclear stain DAPI (Figs. 4–6), and sections were rinsed in PBS ( $3 \times 5$  minutes), mounted on gelatin-subbed slides, and cover-slipped. Adjacent tissue sections were stained for Nissl so that laminar patterns visualized with Nissl stains could be compared with DAPI and NeuN labeling (Fig. 6).

## RESULTS

The weight of the whole brain (including both cortical hemispheres, thalamus, hypothalamus, cerebellum, and brainstem; shown at each age in Fig. 7) significantly increased across development ( $F_{5,27} = 111.88$ ,  $P < 0.0001$ ; see Table 3 for values). Likewise, the weights of the neocortex ( $F_{5,27} = 47.05$ ,  $P < 0.0001$ ), subcortical regions ( $F_{5,27} = 110.47$ ,  $P < 0.0001$ ), and cerebellum ( $F_{4,23} = 40.87$ ,  $P < 0.0001$ ) also significantly increased

across development (Fig. 8A). In contrast, the brain weight/body weight ratio significantly decreased across development ( $F_{5,27} = 69.09$ ,  $P < 0.0001$ ; Fig. 8B), indicating that, although both the body and the brain increased in weight across the life span, the body grew at a much faster rate than the brain.

Different regions of the brain showed differential patterns of growth across development (Fig. 8C). At each age, the proportion of the brain comprising the neocortex, subcortical regions, and cerebellum was determined by dividing the weight of the structure in question by the weight of the whole brain. The proportion of the brain consisting of the neocortex was 7.7% at P18, increasing to 10.2% at P35 and significantly decreasing to 8.0% at P180 and remaining at that level throughout adulthood ( $F_{5,27} = 12.82$ ,  $P < 0.0001$ ; Fig. 8C, Table 3). The proportion of the brain comprising subcortical regions was highest at P18 at 44.0% and by P56 had significantly

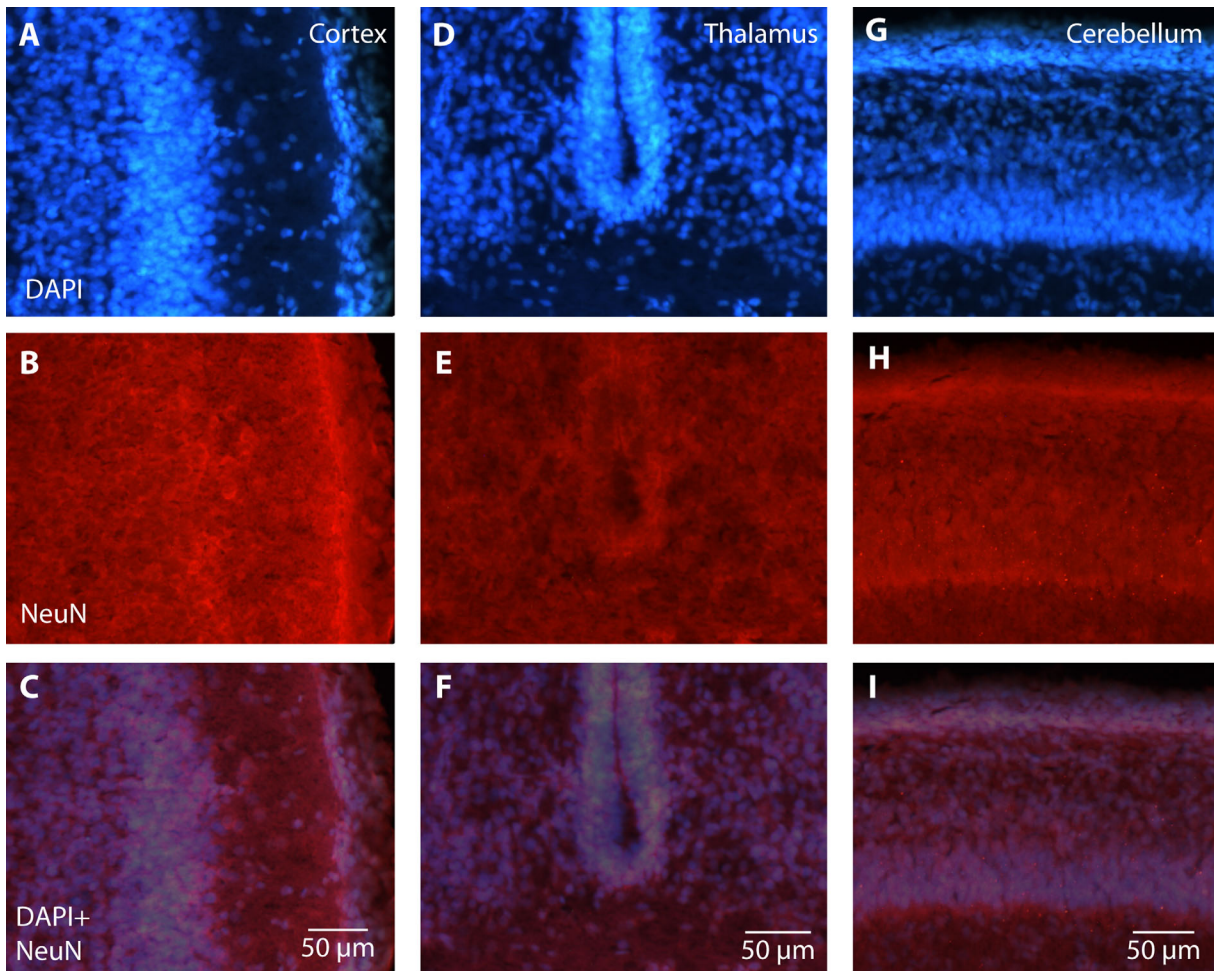


**Figure 5.** The normal, anisotropic distribution of DAPI<sup>+</sup> and NeuN<sup>+</sup> cells in portions of the neocortex (A–C), thalamus (D–F), and cerebellum (G–I) in the brain of a P18 opossum. The superimposition of DAPI<sup>+</sup> (blue; A,D,G) and NeuN<sup>+</sup> (red; B,E,H) cells reveals the distribution of neurons (pink; C,F,I). In these images, the laminar structures of the cortex and cerebellum are clearly identifiable in both the DAPI<sup>+</sup> and the NeuN<sup>+</sup> cells. Within the thalamic section, there is a dense band of DAPI<sup>+</sup> cells surrounding the ventricle. This band can also be seen in the NeuN<sup>+</sup> cells, but it is very faint, indicating that this area contains a large proportion of nonneuronal cells or premitotic cells. Color and contrast have been adjusted in Adobe Photoshop. Scale bars = 50  $\mu\text{m}$ .

decreased to 31.0%, where it remained through >P365 ( $F_{5,27} = 67.93$ ,  $P < 0.0001$ ). The cerebellum, on the other hand, significantly increased from 5.5% at P18 to 12.4% at P56 ( $F_{5,27} = 26.48$ ,  $P < 0.05$ ). These data indicate that, although the brain grows steadily during the early part of the life span, it does not grow uniformly.

To demonstrate the relationship between DAPI and NeuN stains and the efficacy of NeuN in labeling neurons in both very young and adult brains, the distribution of cells and neurons was visualized by staining whole sections of P18 and P180 tissue (Figs. 4–6). All cells were labeled using DAPI (Fig. 4A,D,G), and the tissue was counterstained for NeuN to identify neurons (Fig. 4B,E,H). The superimposition of the DAPI<sup>+</sup> and NeuN<sup>+</sup> images in Figure 4C,F,I allowed us to visualize individual nuclei and neurons and distinguish them from nonneuronal cells.

The relationship between DAPI and NeuN also was demonstrated in the P18 opossum (Fig. 5), and for the neocortex DAPI and NeuN labeling were directly compared with adjacent Nissl-stained sections (Fig. 6). Both the P18 and the P180 tissue showed a laminar distribution of neurons in the cortex and cerebellum. In the developing neocortex, laminar patterns, as revealed with both Nissl and DAPI stains, indicated an abundance of cells in the ventricular zone and subventricular zones, although few of these cells were NeuN positive (Fig. 6A–C). Some NeuN-positive cells were labeled in the subplate, and NeuN-positive cells were found in abundance in the cortical plate. In the adult, Nissl- and DAPI-stained sections appeared similar, showing a similar laminar distribution with a prominent layer 2–3 (Fig. 6D,E), and NeuN revealed an abundance of neurons in these same layers

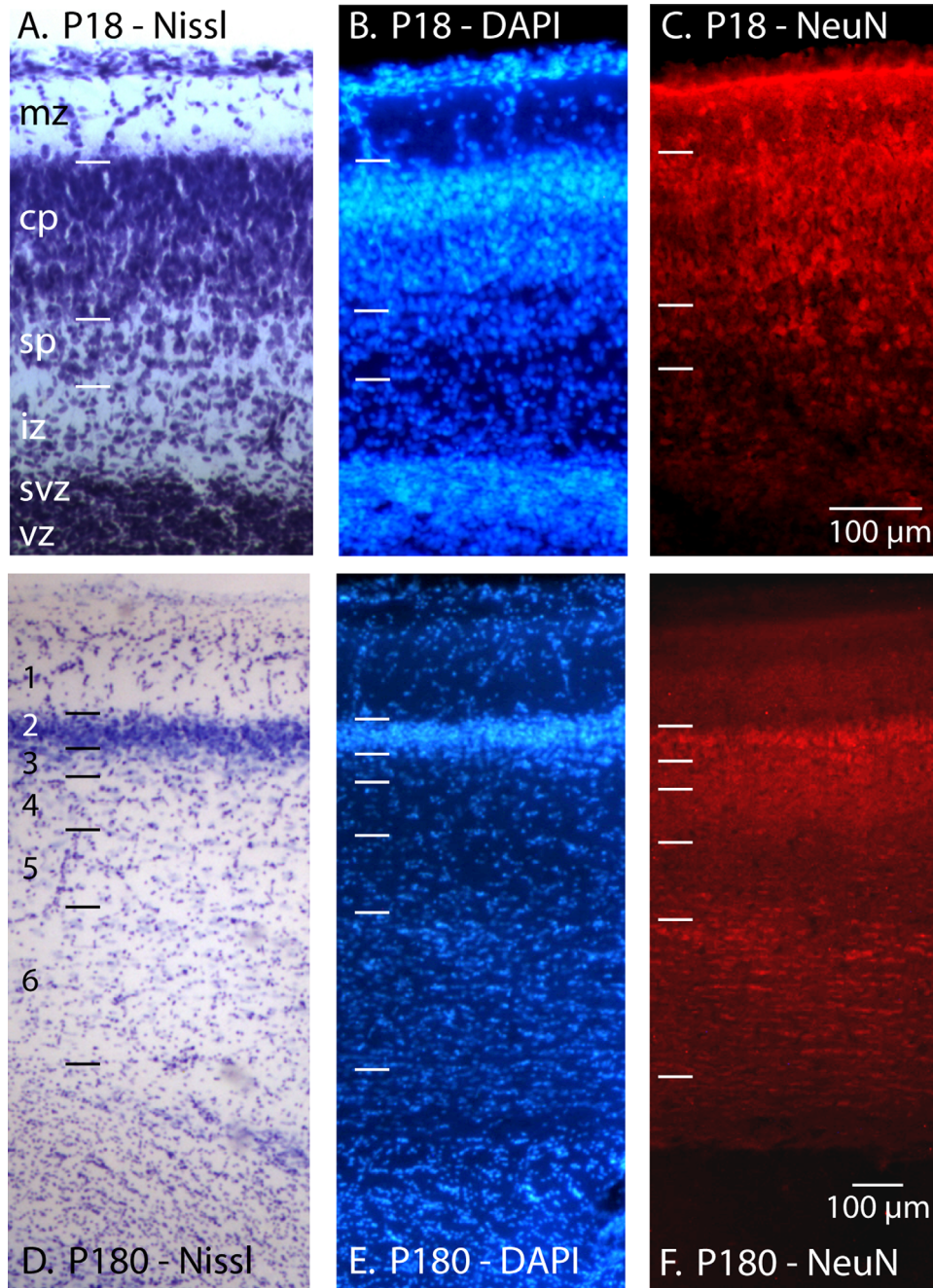


**Figure 6.** The normal, anisotropic distribution of cells in cortical tissue stained for Nissl (A,D), DAPI (B,E), and NeuN (C,F) in P18 (A–C) and P180 (D–F) opossums. Both the P18 and P180 cortical sections are from a similar location in somatosensory cortex. At P18 the laminar organization of the developing neocortex is distinct, and neurons within the cortical plate are clearly labeled with NeuN. Although the ventricular zone is cell dense, it contains no NeuN-labeled cells. In the adult the characteristic layers of the neocortex are visible in both Nissl- and DAPI-stained tissue. Tissue stained for NeuN indicates a lack of neurons in layer 1, dense labeling of neurons in layers 2–3, and moderate labeling of neurons in layer 4 and 6. mz, Marginal zone; cp, cortical plate; sp, subplate; iz, intermediate zone; svz, subventricular zone; vz, ventricular zone. Laminal divisions of early postnatal animals have been described by Cheung et al. (2010) and Saunders et al. (1989). Color and contrast have been adjusted in Adobe Photoshop. Scale bars = 100  $\mu\text{m}$ .

(Fig. 6D,E). Moderate numbers of neurons were observed in deeper cortical layers (Fig. 6F).

The isotropic fractionator method utilizes these same fluorescent stains and follows the same principle of

identifying neurons within a population of cells, but it homogenizes the tissue, making different structures of the brain (e.g., neocortex, cerebellum) isotropic. In this way, the cellular composition of large pieces of neural

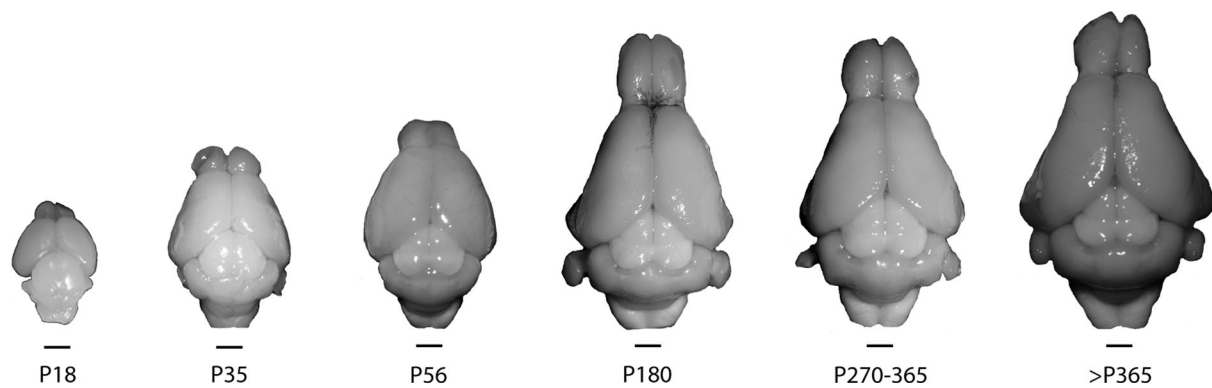


**Figure 7.** Relative size of *Monodelphis domestica* brains at P18, P35, P56, P180, P270–365, and >P365. The size and shape of the brain change dramatically during the first 6 months of life. The caudolateral expansion of the cerebral cortex is particularly apparent. After sexual maturity (P180), there is little change in the size of the entire brain or the relative size of different structures. Images were converted to gray scale and contrast and brightness levels were adjusted in Adobe Photoshop. Scale bars = 2 mm.

**TABLE 3.**  
Weights of Brain Regions

Age	Whole brain	Neocortex	Subcortical regions	Cerebellum
P18	0.1191 ± 0.0026	0.0092 ± 0.0004	0.0525 ± 0.0014	0.0066 ± 0.0009
P35	0.3450 ± 0.0176	0.0353 ± 0.0031	0.1401 ± 0.0055	0.0375 ± 0.0042
P56	0.5112 ± 0.0062	0.0498 ± 0.0024	0.1586 ± 0.0060	0.0498 ± 0.0011
P180	0.8949 ± 0.0568	0.0719 ± 0.0057	0.2767 ± 0.0142	0.1174 ± 0.0085
P270–365	0.8533 ± 0.0404	0.0685 ± 0.0038	0.2705 ± 0.0142	0.1148 ± 0.0068
>P365	0.9833 ± 0.0272	0.0726 ± 0.0029	0.3096 ± 0.0072	0.1235 ± 0.0070

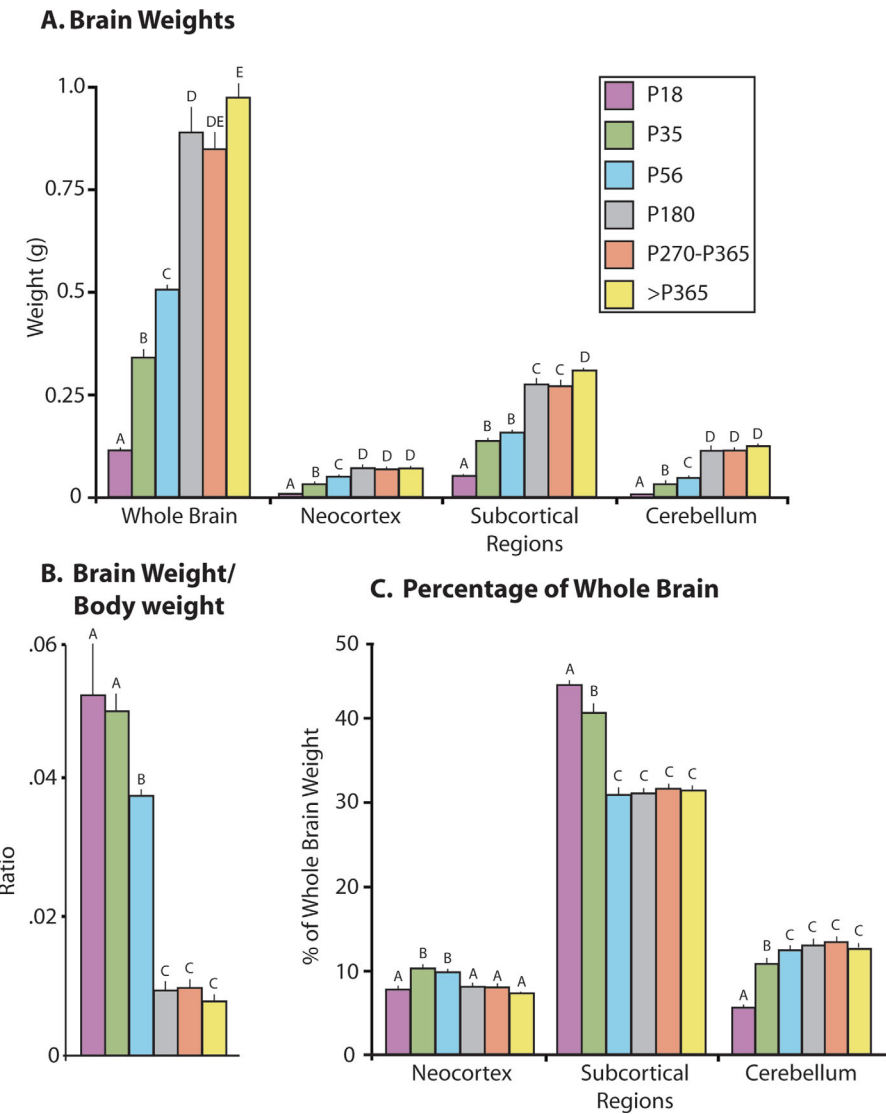
Age	Brain weight/ body weight
P18	0.0522 ± 0.0087
P35	0.0503 ± 0.0031
P56	0.0382 ± 0.0011
P180	0.0102 ± 0.0010
P270–365	0.0100 ± 0.0011
>P365	0.0080 ± 0.0004

Age	% Neocortex	% Subcortical regions	% Cerebellum
P18	7.72 ± 0.33	44.05 ± 0.36	5.52 ± 0.17
P35	10.18 ± 0.44	40.73 ± 1.06	10.75 ± 0.80
P56	9.73 ± 0.41	31.00 ± 0.86	12.40 ± 0.21
P180	8.01 ± 0.22	31.03 ± 0.52	13.15 ± 0.55
P270–365	8.03 ± 0.27	31.69 ± 0.43	13.44 ± 0.39
>P365	7.26 ± 0.29	31.51 ± 0.36	12.57 ± 0.66

tissue can be quantified. It should be noted, however, that during the course of the homogenization areal and laminar information is necessarily lost. After the homogenization of the tissue and nuclear dissociation, all nuclei were first labeled with DAPI, then counterstained for NeuN in order to reveal neuronal nuclei (Fig. 3). In Figures 3–6 nonneuronal nuclei are visualized as blue, neuronal nuclei are visualized as red, and nuclei that stain for both DAPI and NeuN are visualized as pink.

The cellular composition of the neocortex changed significantly across development (Fig. 9). The total number of cells in the neocortex significantly increased across development ( $F_{5,27} = 7.19$ ,  $P < 0.001$ ; Fig. 9A). Although the total number of neurons did not significantly change ( $F_{5,27} = 0.27$ , NS), the total number of nonneurons significantly increased ( $F_{5,27} = 15.68$ ,  $P < 0.0001$ ). Furthermore, the overall cell density decreased across development ( $F_{5,27} = 72.31$ ,  $P < 0.0001$ ; Fig. 9B), as did



**Figure 8.** Changes in brain weight (A), brain/body ratios (B), and relative size of major structures (C) across development. The entire brain and major structures increase in size until P180 and then remain relatively constant (A). Brain and body weight ratios decrease with age and then stabilize at P180, indicating that the body grows at a much faster rate than the brain until sexual maturity (B). The major structures that compose the brain undergo different trajectories of growth (C). Mean  $\pm$  SE. Values with different letters are significantly different.

neuronal density ( $F_{5,27} = 23.13, P < 0.0001$ ) and non-neuronal density ( $F_{5,27} = 6.50, P < 0.001$ ). The neuron percentage (i.e., the percentage of total nuclei that were positive for NeuN) significantly decreased across development ( $F_{5,27} = 3.10, P < 0.05$ ; Fig. 9C; Table 4).

For subcortical regions, the cellular composition also significantly changed across development (Fig. 10). The total number of cells significantly increased with age ( $F_{5,27} = 20.06, P < 0.0001$ ; Fig. 10A; Table 4). Neuronal number was greatest at P18, during neurogenesis, and then significantly decreased with age ( $F_{5,27} = 3.48, P < 0.05$ ), whereas the total number of nonneurons significantly increased over the same period ( $F_{5,27} = 43.62,$

$P < 0.0001$ ). The overall cell density significantly decreased across development ( $F_{5,27} = 5.13, P < 0.005$ ; Fig. 10B), as did neuronal density ( $F_{5,27} = 74.01, P < 0.0001$ ), although the density of nonneurons increased ( $F_{5,27} = 27.51, P < 0.0001$ ). The percentage of neurons significantly decreased throughout the life span ( $F_{5,27} = 157.73, P < 0.0001$ ; Fig. 10C).

The cerebellum also showed significant changes in its cellular composition across development (Fig. 11). The total number of cells sharply and significantly increased until P180, and then decreased through  $>P365$  ( $F_{5,23} = 30.43, P < 0.0001$ ; Fig. 11A, Table 4). The total number of neurons did not significantly change across

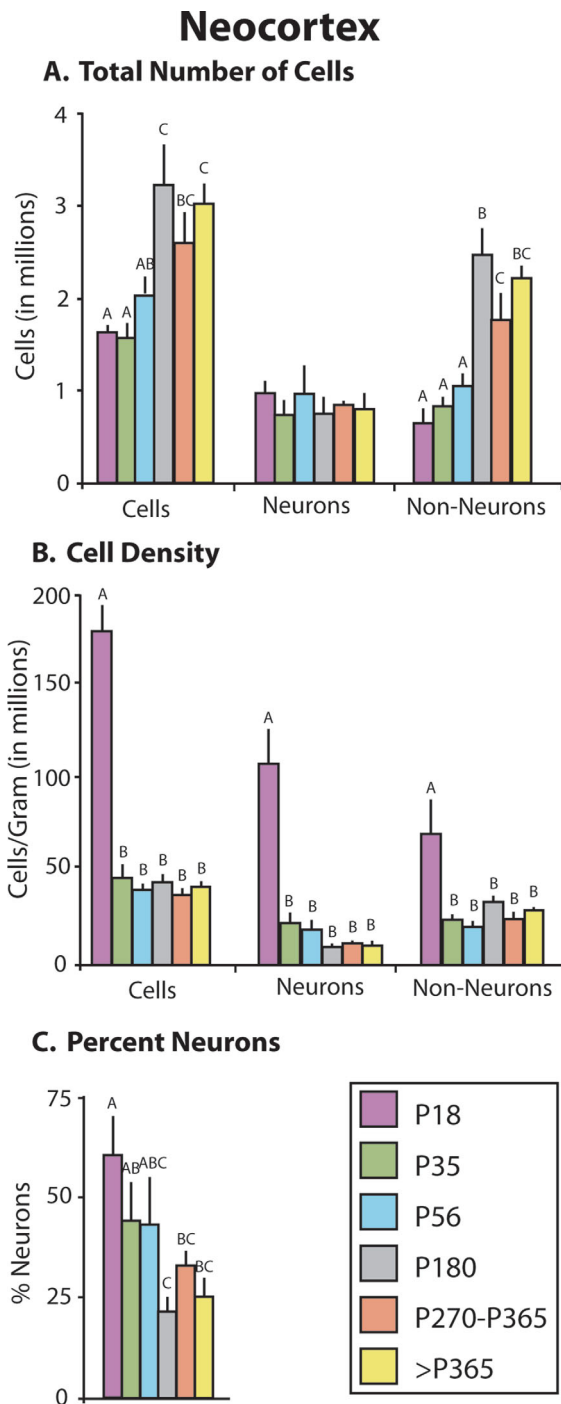


**Figure 9.** Changes in cellular composition of the neocortex. (A) Changes in the total number of cells (left), number of neurons (center), and number of nonneurons (right) in the neocortex at different developmental stages. Although the total number of cells and nonneurons increases across the ages we sampled, the number of neurons does not change. (B) Changes in total cell density (left), neuronal density (center), and nonneuronal density (right) across development. The density of both cell types was highest at P18, decreased by P35, and then remained unchanged through adulthood. (C) The percentage of all cells within the neocortex that were neurons decreased across development. Mean  $\pm$  SE. Values with different letters are significantly different.

development ( $F_{5,23} = 2.45$ ,  $P = 0.07$ ), but the total number of nonneurons significantly increased until P180, at which point it remained steady ( $F_{5,23} = 44.36$ ,  $P < 0.0001$ ). Cell density increased from P18 through P35 and then gradually and significantly decreased with age ( $F_{5,23} = 5.43$ ,  $P < 0.005$ ; Fig. 11B). In contrast, neuron density significantly decreased across development ( $F_{5,23} = 6.46$ ,  $P < 0.005$ ), and the nonneuron density increased from P18 to P35, then decreased from P35 to  $>P365$  ( $F_{5,26} = 15.26$ ,  $P < 0.0001$ ). Finally, similar to both the neocortex and the subcortical regions, the percentage of neurons within the cerebellum significantly decreased with age ( $F_{5,27} = 23.72$ ,  $P < 0.0001$ ; Fig. 11C).

## DISCUSSION

The current study showed that the size of the body and brain increased with age, and the ratio between the brain and the body was relatively high early in development, but both dropped at 6 months of age and remained constant. In terms of cellular composition, the total number of cells in the neocortex, subcortical structures, and cerebellum increased with age until 6 months. However, there were some important differences in the growth patterns and cellular composition across the major structures, particularly with regard to neuronal number. For example, in the neocortex, the cellular density was highest at P18, dropped off at P35, and remained constant across progressively older age groups. The number of neurons remained relatively constant, whereas the percentage of neurons declined with age (Figs. 9, 12) suggesting that the growth of the neocortex is due to the addition of non-neuronal cells and that naturally occurring neuronal cell death occurs before P18 or is not prevalent in the developing marsupial neocortex. The increase in nonneuronal cells is not surprising, in that our earliest sampled age (P18) was during peak cortical neurogenesis, which is then followed by gliogenesis within the neocortex (Cheung et al., 2010; Miller and Gauthier, 2007; Puzzolo and Mallamaci, 2010). In subcortical regions, neuron number was high at P18, decreased at P35, and remained constant at progressively older ages, as did the percentage of neurons; a converse relationship was observed for nonneuronal cells. Neuronal density and percentage neurons also dropped significantly at P35 compared with P18, and a converse relationship was observed for non-neuronal cells. Finally, in the cerebellum, cell number increased with age and was accounted for mainly by an increase of nonneuronal cells. As in the cortex, neuronal number remained constant across all ages. The density and percentage of neurons decreased dramatically after P18, and a converse relationship in cell density was observed for nonneuronal cells.

**TABLE 4.**  
Cellular Composition of Brain Regions

Age	% Neurons	No. cells (in millions)	No. neurons (in millions)	No. nonneurons (in millions)	No. cells/gram (in millions)	No. neurons/gram (in millions)	No. nonneurons/gram (in millions)
<b>Neocortex</b>							
P18	60.55 ± 9.44	1.637 ± 0.058	.985 ± 0.139	.653 ± 0.163	180.032 ± 13.690	109.054 ± 18.773	70.977 ± 18.490
P35	44.44 ± 9.21	1.580 ± 0.141	.743 ± 0.093	.836 ± 0.093	47.043 ± 6.952	22.792 ± 5.787	24.250 ± 3.103
P56	43.52 ± 11.69	2.027 ± 0.220	.970 ± 0.131	1.057 ± 0.131	40.454 ± 3.142	19.059 ± 6.024	21.394 ± 2.928
P180	22.04 ± 3.63	3.224 ± 0.440	.748 ± 0.283	2.476 ± 0.283	44.578 ± 4.136	10.111 ± 2.132	34.468 ± 2.678
P270–365	33.55 ± 3.71	2.606 ± 0.308	.847 ± 0.050	1.760 ± 0.306	37.901 ± 3.146	12.509 ± 1.226	25.391 ± 3.297
>P365	25.62 ± 4.86	3.030 ± 0.209	.803 ± 0.199	2.227 ± 0.120	42.067 ± 2.623	10.917 ± 2.545	30.779 ± 1.675
<b>Subcortical regions</b>							
P18	77.40 ± 5.00	3.184 ± 0.185	2.486 ± 0.267	.698 ± 0.117	60.693 ± 3.293	47.436 ± 5.288	13.257 ± 2.198
P35	6.77 ± 2.67	7.187 ± 0.659	.503 ± 0.199	6.684 ± 0.610	51.355 ± 4.339	3.789 ± 1.677	47.565 ± 3.351
P56	6.17 ± 0.69	8.240 ± 0.287	.512 ± 0.066	7.728 ± 0.252	52.090 ± 1.759	3.186 ± 0.286	48.904 ± 1.868
P180	6.30 ± 0.99	12.496 ± 1.009	.803 ± 0.151	11.693 ± 0.912	44.941 ± 1.637	2.868 ± 0.498	42.073 ± 1.344
P270–365	4.55 ± 0.32	12.073 ± 1.043	.556 ± 0.079	11.517 ± 0.971	44.636 ± 3.108	2.053 ± 0.277	42.582 ± 2.853
>P365	7.25 ± 0.90	13.147 ± 6.223	.959 ± 0.172	12.044 ± 0.632	42.577 ± 2.326	3.079 ± 0.510	38.885 ± 2.541
<b>Cerebellum</b>							
P18	86.93 ± 4.55	1.613 ± 0.135	1.392 ± 0.103	.221 ± 0.084	245.857 ± 21.530	212.595 ± 17.028	33.262 ± 12.790
P35	19.31 ± 8.14	14.874 ± 0.635	2.740 ± 1.051	12.134 ± 1.521	416.778 ± 46.719	90.409 ± 49.516	326.368 ± 33.137
P56	30.82 ± 5.67	24.155 ± 1.896	5.794 ± 1.732	18.36 ± 1.039	374.539 ± 31.199	90.037 ± 27.103	284.501 ± 5.000
P180	12.75 ± 4.20	36.835 ± 3.654	5.122 ± 1.889	31.713 ± 2.399	314.390 ± 22.527	43.320 ± 16.131	271.070 ± 12.177
P270–365	9.97 ± 6.32	32.893 ± 2.282	1.258 ± 0.401	31.363 ± 1.914	279.857 ± 21.313	10.702 ± 3.633	269.154 ± 17.996
>P365	8.45 ± 4.5	30.348 ± 2.903	1.275 ± 0.342	29.073 ± 2.650	239.780 ± 17.196	9.953 ± 2.703	229.827 ± 15.117

It should be noted that NeuN is a marker for postmitotic neurons (Mullen et al., 1992; Sarnat et al., 1998). That is, NeuN is not expressed in neuronal precursor cells but is expressed as the neurons exit the cell cycle (Martinez-Cerdeno et al., 2012; Noctor et al., 2008; Oomman et al., 2004; Yan et al., 2001). Thus, the large proportion of NeuN-positive cells during early development was not a result of labeling blastocysts or other immature cell types.

Several important caveats must be considered when interpreting data that use NeuN as a neuronal marker in

different tissue and in different species. First, NeuN fails to label several types of neurons in the adult brain, such as mitral cells in the olfactory bulb, retinal photoreceptors, and Purkinje cells in the cerebellum (Mullen et al., 1992). Second, NeuN fails to label some groups of postmitotic neurons, such as layer VIa cells in the neocortex (Lyck et al., 2007) and nongranule cell interneurons in the mouse cerebellum (Weyer and Schilling, 2003) until later developmental ages. The latter investigation also indicates that the expression of NeuN during development may be dependent on the physiological status of the developing neurons (Weyer and Schilling, 2003). Thus, studies that utilize NeuN to examine patterns of cellular composition across multiple developmental time points must be interpreted with caution. Finally, although there is good evidence that NeuN labels neurons in adult mammalian nervous tissue, and the use of the isotropic fractionator methodology in over 30 species, including capybaras, star-nosed moles, bonnet macaques, and baboons, is based on this assumption (see, e.g., Burish et al., 2010; Collins et al., 2010a; Herculano-Houzel et al., 2006; Sarko et al., 2009), it is likely that species-specific differences in its labeling pattern exist. For example, NeuN does not label substantia nigra neurons in the gerbil but does label these neurons in rats (Kumar and Buckmaster, 2007). Thus, comparative studies on specific details of its labeling patterns for species other than mice and rats are important for accurate interpretation of data from this methodology.

An example of how these issues impact our own investigation comes from our estimates of neuronal and non-neuronal populations in the cerebellum where the numbers are low compared with other species. As noted above, NeuN does not label Purkinje cells in the adult cerebellum and may not label all interneurons in the cerebellum or layer 6 cortical neurons until later developmental

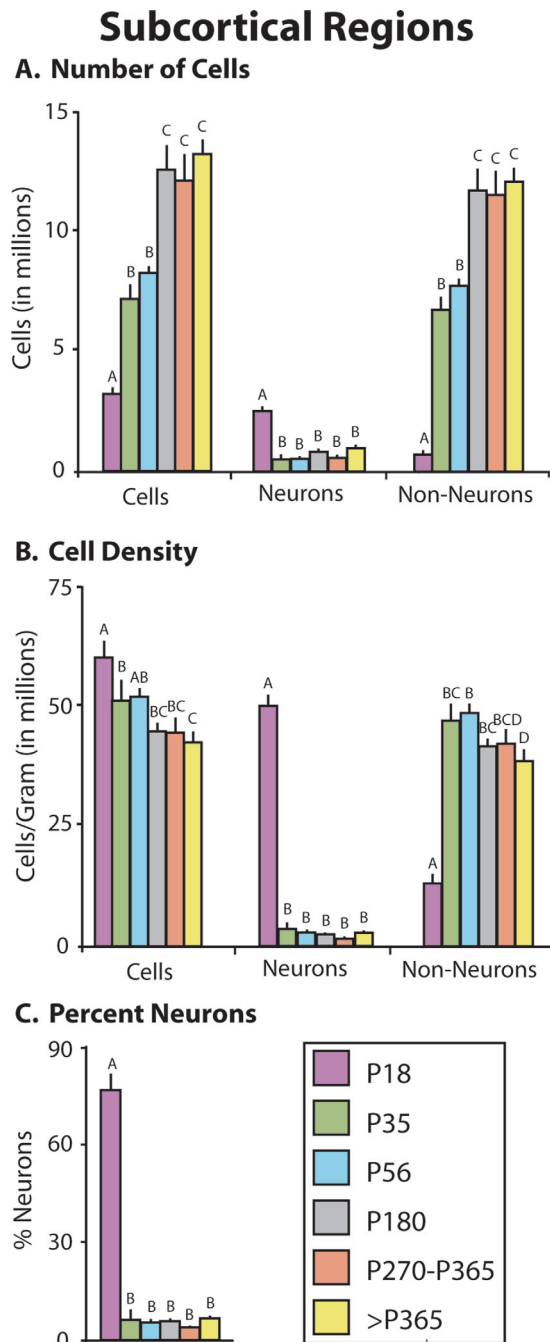
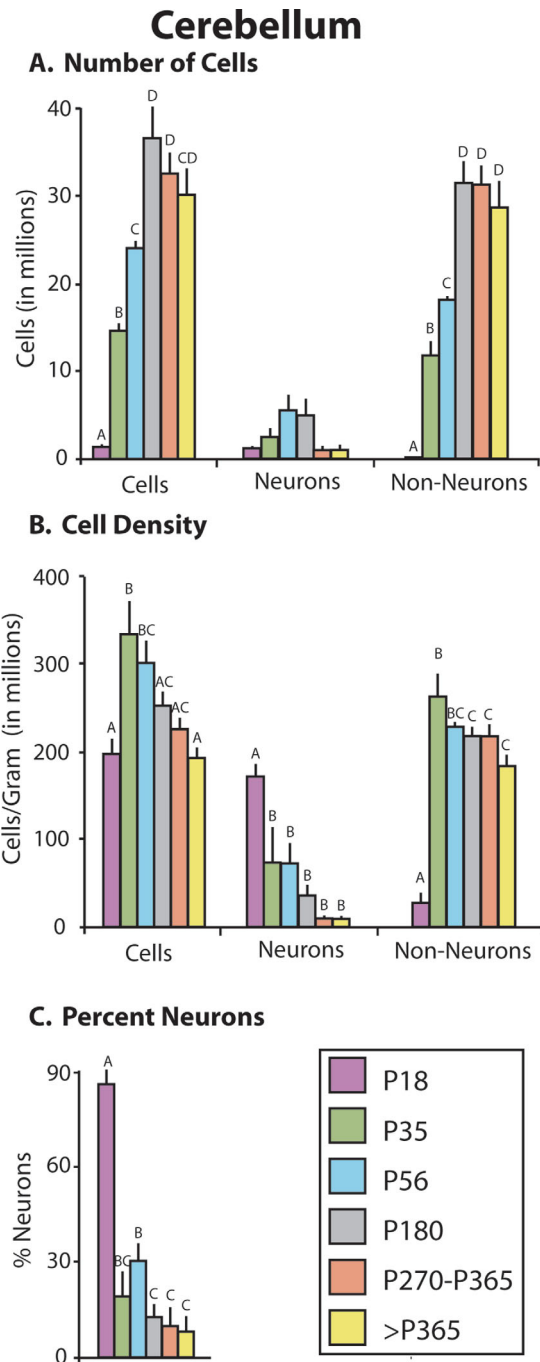


Figure 10

**Figure 10.** Changes in cellular composition of subcortical regions. (A) Changes in the total number of cells (left), number of neurons (center), and number of nonneurons (right) in the neocortex at different developmental stages. The total number of cells and nonneurons increased across development, but the number of neurons was highest at P18, decreased by P35, and remained unchanged across development. (B) Changes in the total cell density (left), neuronal density (center), and nonneuronal density (right) across development. The total cell density and neuronal density were highest at P18. Although the total cell density gradually decreased across development, neuronal density decreased dramatically by P35 and thereafter remained constant. In contrast, nonneuronal density was lowest at P18, increased by P35, then decreased slightly throughout adulthood. (C) The percentage of neurons was highest at P18, significantly decreased by P35, and remained constant across development. Mean  $\pm$  SE. Values with different letters are significantly different.



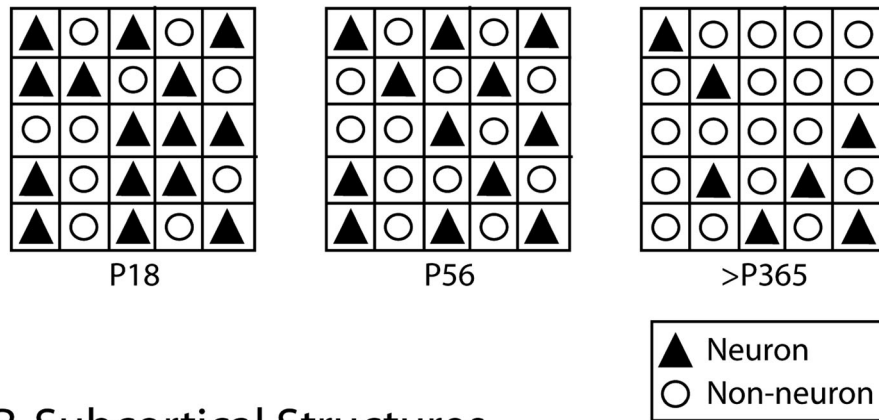
**Figure 11.** Changes in cellular composition of the cerebellum. (A) Changes in the total number of cells (left), number of neurons (center), and number of nonneurons (right) in the neocortex at different developmental stages. The total number of cells significantly increased from P18 through P180, then decreased through >P365. The number of neurons did not significantly change across development. In contrast, the number of nonneurons increased from P18 through P180, then remained constant. (B) Changes in the total cell density (left), neuronal density (center), and nonneuronal density (right) across development. Both total cell density and nonneuronal density increased from P18 to P35, then decreased through >P365. In contrast, neuronal density was highest at P18, then decreased through adulthood. (C) The percentage of neurons decreased across the life span. Mean  $\pm$  SE. Values with different letters are significantly different.

ages. If this is the case for *Monodelphis*, then, at earlier development ages, neurons in these structures may be underrepresented. However, the low numbers of cells in the developing cortex and cerebellum in the developing *Monodelphis* are also observed in adults, suggesting that there may be true species differences in marsupials and small-brained eutherian mammals. These differences are discussed below.

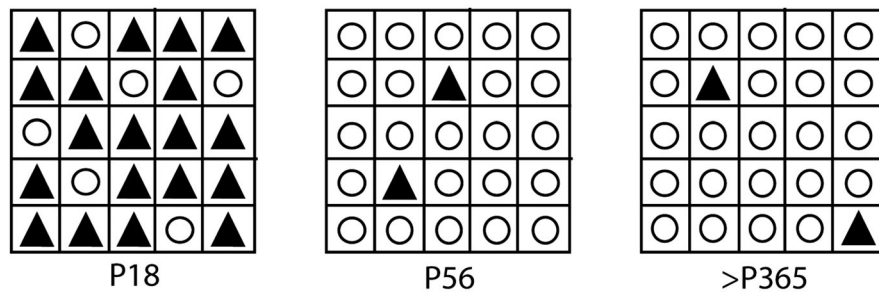
### Neural development in marsupials and rodents

Although this is the first study in marsupials to examine and quantify the cellular composition across major neural structures through different developmental time points, there are other studies of neural development in marsupials, particularly in the neocortex. As in other mammals, neurogenesis in the marsupial neocortex occurs in a rostro-lateral to medio-caudal progression (Molnar et al., 1998; Sanderson and Weller, 1990). In marsupials, this process is prolonged and occurs almost completely postnatally, and, in some marsupials, such as the native cat, brush-tailed possum, and wallaby, it occurs over a 2–3-month postnatal period (Aitkin et al., 1991; Marotte and Sheng, 2000; Sanderson and Weller, 1990). Neurogenesis and gliogenesis have been examined specifically in *Monodelphis* as well, and their duration may be somewhat shorter than in Australian marsupials (Puzzolo and Mallamaci, 2010). From bromodeoxyuridine (BrdU) pulse-chase birth-dating analysis, Puzzolo and Mallamaci suggest that neurogenesis was complete by P16. Neurons born after P18 remain mostly beneath the cortical plate; ages past P18 were not examined. By P30 cells born at P16 have migrated to the superficial layers of the neocortex, indicating that the laminar development of the neocortex is complete. It should be noted that the samples in this previous study were taken from midfrontal cortex, where the wave of neurogenesis begins and ends earlier than in other portions of the neocortex. Other studies examining development of the neocortex in *Monodelphis* indicate that cortical neurogenesis occurs over a longer postnatal period; that the characteristic developmental layers, including the ventricular zone and subventricular zone, are still clearly apparent at P45 (Saunders et al., 1989); and that late-stage neurogenesis occurs in the middle of the fourth postnatal week (Molnar et al., 1998). Our own data indicate that peak neurogenesis of the neocortex and subcortical structures is complete by P35, because neuronal number is relatively constant across ages sampled for the neocortex (P18 to adulthood), and decreases at P35 for subcortical structures. Our studies also indicate that gliogenesis is prolonged in all structures of the brain that were examined and extends into the sixth postnatal month of life (P180).

## A. Neocortex



## B. Subcortical Structures



## C. Cerebellum

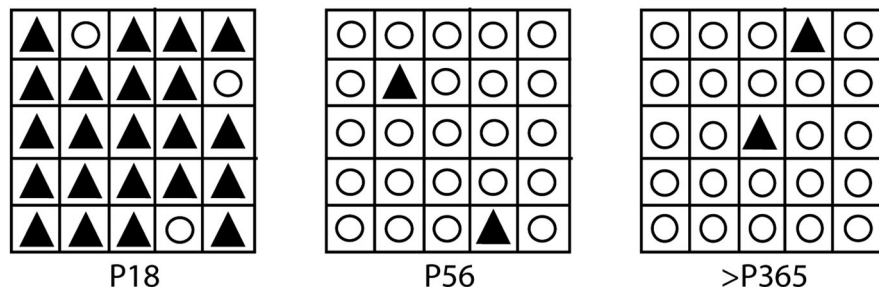


**Figure 12.** Diagram of changes in cellular composition across development. The major assumption here is that cells (neuronal and non-neuronal) occupy the entire structure and that cell size does not change dramatically. This assumption is purposely simplified to emphasize better the changes in number and density of cells across development. Each outer square represents a set volume of tissue for each age group. Neurons are represented by triangles, and nonneurons are represented by circles. The ratio of neurons to nonneurons follows a distinct developmental trajectory in each brain region. (A) In the neocortex, the total number of cells increases with the overall size of the structure. However, the number of neurons remains constant from P18 through adulthood. Thus, as the size of the structure increases, the neuronal density decreases. (B) In the subcortical structures, the total number of cells is lowest at P18, but the total number of neurons is highest at that age, resulting in a high neuronal density. Throughout development, the number of neurons decreases as the total number of cells increases, resulting in a significantly lowered neuronal density. (C) In the cerebellum, the total number of cells is lowest at P18, but, because a large proportion of those cells is neuronal, we see a very high neuronal density. The number of neurons remains constant throughout development into adulthood, but the number of cells (nonneurons) increases, resulting in a lower neuronal density. All diagrams are based on the total cell density and neuronal density of brain regions at P18, P56, and < P365.

There are only two other studies in which cellular composition of the brain has been examined across developmental age groups: one in mice (Lyck et al., 2007) and

one in rats (Bandeira et al., 2009). The former study only examined the neocortex. However, neither of these studies captured early embryonic stages, for which it has

been reported that the vast majority of cortical and sub-cortical neurons are generated in mice and rats (Dehay and Kennedy, 2007; Robinson and Dreher, 1990). In rats cortical neurogenesis begins on E12 and ends on E21, and in mice cortical neurogenesis begins on E11 and ends on E19. These dates correspond to E12 and P24, respectively, in *Monodelphis*. Thus, the only data from the current study that we can compare with these previous studies would be at P35 and progressively later stages.

Probably the most notable difference between the current study and these previous investigations is our observation that the number of cortical neurons stabilizes or declines following the completion of neurogenesis as defined in earlier studies (see above), whereas these previous studies in mice and rats (Bandeira et al., 2009; Lyck et al., 2007) show a twofold or more increase in the number of neurons that occurs at P5 in the rat and P16 in the mouse, well after most studies indicate that neurogenesis has ended. These studies also demonstrate that this initial increase in neurons is followed by a reduction in neurons at later postnatal ages. In rats this reduction is as large as 70%.

Although other authors have reported postnatal neurogenesis of GABAergic neurons in mice, the number of these neurons that actually migrate to the neocortex was estimated to be relatively modest (Inta et al., 2008). Lyck and colleagues (2007) suggest that this increase in the number of neurons in postnatal mice could come from neurons migrating into the neocortex from other regions such as the telencephalic wall (Molyneaux et al., 2005; Noctor et al., 2004) and medial ganglionic eminence (Anderson et al., 1997; Kriegstein and Noctor, 2004; Wichterle et al., 2001). Bandiera and colleagues (2009) ascribe increases in neuronal population to massive postnatal neurogenesis, a notion counter to all that we know about neurogenesis in rodents; in fact, their data suggest that most of neurogenesis occurs postnatally. However, given the limitation of the methods and the variable efficacy of NeuN for labeling particular populations of neurons and neurons present at early developmental ages (see above), it is not possible to determine whether the cells that the authors encountered at these early postnatal stages are newly born cells, migrating cells or cells that had not previously expressed NeuN at these earlier ages. The methods used for the rat suggest but do not specify that the pyriform cortex was included as part of the neocortex, which could also account for some of the differences described (Bandeira et al., 2009).

The cerebellum differs from the other brain regions described here in that at P18 it makes up only a small proportion of the weight of the whole brain (5.52%) and that proportion more than doubles by the time the opossum reaches adulthood (13.15% at P180; Figs. 6, 7, Table

3). Structurally, at P18, the opossum cerebellum is very immature, consisting of only an external granular layer, but, by P35, all of the cerebellar layers are apparent, including the external granular, molecular, and internal granular layers as well as white matter (Sanchez-Villagra and Sultan, 2002). This late growth pattern is similar to that seen in rats, in which the vast majority of cerebellar growth, including the development of its characteristic fissures and folia, occurs postnatally (Bandeira et al., 2009; Carletti and Rossi, 2008; Goldowitz and Hamre, 1998).

As noted above, the number of cerebellar neurons in *Monodelphis* throughout all stages of development, including adults, is low compared with that in eutherian mammals. This may be due in part to a lack of labeling of Purkinje cells, lack of labeling of nongranule cell interneurons (at least at earlier stages), lack of efficacy of labeling cerebellar cells other than the Purkinje cells, or true species differences. If our small number of cerebellum neurons in adults is due to a lack of Purkinje cell labeling, and if the ratio of Purkinje cells to granule cells is similar to that estimated for mice (Goldowitz and Hamre, 1998; Wetts and Herrup, 1983), then our results would have underestimated the number of neurons in the cerebellum by less than 1%.

### Cellular composition of the neocortex in other small-brained animals

Another important difference between the current study and previous studies utilizing similar techniques is that there are an extremely small number of neurons that compose the adult marsupial brain compared with estimates from other small-brained mammals such as mice (Lyck et al., 2007), shrews, and moles (Sarko et al., 2009). For example, in adult mice, the neocortex contains 14.4 million cells; about 50% are neurons and 50% are glial cells. Shrews and moles demonstrate a similarity in the composition of cells within the neocortex; the number of cells in the small neocortex (0.7 g) of the smoky shrew was 14 million. As in mice, neurons made up about 50% of these cells. As the size of the neocortex increased in shrews and moles, the proportion of neurons to nonneurons changed, with larger brained insectivores having a greater percentage of nonneurons (e.g., 78% in the hairy-tailed mole; see Sarko et al., 2009; Table 1), which is similar to the percentage of nonneurons that we observed in adult opossums.

The total number of cells in an adult *Monodelphis* neocortex (0.7 grams) was 3.2 million; 750,000 or 22% were neurons and 2.5 million (78%) were nonneurons. Thus, both the total number of cells and the proportions of neurons vs. nonneurons were dramatically different from the

case in rodents and insectivores with a similarly sized neocortex. This suggests that there may be fundamental differences in signal processing and transmission in marsupial brains and that glia may play a more important role in information processing in marsupials compared with eutherian mammals (see below). No other studies have examined the cellular composition of marsupial brains, so it is not known whether this observation on overall number as well as proportion of neurons to nonneurons is a general characteristic of marsupials or is specific to *Monodelphis*.

However, if this were a general feature of marsupials, it would suggest that early mammals had brains that were composed of substantially fewer neurons and that glial cells might have played a more central role in processing. Changes in the proportion of neurons (increases in number and density) might have arisen in eutherian mammals along with more neuron-centered processing networks. Given the potential role of glial cells in synaptic transmission (see below), this also suggests that the neocortex of early mammals might have had a greater capacity for plastic changes in the adult.

### Benefits and limitations the isotropic fractionator method

When considering data generated using the isotropic fractionator method, it is important to consider both the benefits of this technique and its limitations. Although isotropic fractionator methodology does not replace traditional stereological methods for quantifying various aspects of neuroanatomical organization and development, it offers the extraordinary advantage of estimating the number and composition of cells in the entire brain or entire neural structure in a relatively rapid, consistent manner. Not since the analogous comparative brain morphometry studies of Stephan and colleagues (Baron et al., 1990; Frahm et al., 1982; Stephan et al., 1981) have critical and extensive cross-species comparisons been possible. These early morphometry studies of gross brain organization and size generated numerous and important theories regarding brain scaling in mammals (Finlay and Darlington, 1995; Stevens, 2001). Similarly, isotropic fractionator techniques have been used to compare cellular composition and generate data-driven theories of cellular evolution and brain scaling in a variety of mammals, including several primates (Collins et al., 2010a), different rodents (Herculano-Houzel et al., 2006), shrews and moles (Sarko et al., 2009), and now marsupials. This accumulation of cross-species data serves as an important data repository for any number of neurocomputational, developmental, and evolutionary studies.

Of course, the most obvious limitation of the technique when used in large structures as a whole is the decon-

struction of tissue to rapidly and accurately estimate the number of cells, neurons and nonneurons, that make up a structure. Thus, laminar divisions as well as cortical and nuclear divisions are lost. Second, there is some destruction of nuclei as a result of the homogenization process as well as some loss of nuclei during the immunohistochemical processing of the tissue; however, this loss is estimated to be minimal (Collins et al., 2010b; Herculano-Houzel and Lent, 2005). Furthermore, as mentioned above, there are selected neuron types that NeuN does not label (Mullen et al., 1992), and the efficacy of NeuN has not been well characterized in the brains of the many different animals in which the isotropic fractionator technique has been used. These limitations must be considered when interpreting data.

Finally, as we have already mentioned, the isotropic fractionation method uses dissociated cellular nuclei to generate data concerning the number and density of cells within a structure. Because all the cell membranes, axons, and dendrites have been removed during the cellular dissociation process, this technique cannot provide any concrete information about the size, shape, extracellular spaces, or connections of whole cells and neurons.

### What about glial cells?

The current discussion is based on the assumption that the nonneuronal cells are predominantly glial cells. The other types of cells that constitute the nonneuronal group, endothelial cells, mesothelial cells, and ependymal cells, are relatively restricted in their distribution. Endothelial cells form the thin lining of blood vessels and compose the blood-brain barrier. The mesothelial cells make up the pia mater, which in lissencephalic brains is relatively small compared with the volume of tissue that it encloses. The ependymal cells line the ventricles, whose membrane volume is substantially smaller than cortical gray matter. Thus, among the nonneuronal cell types, glial cells represent the vast majority of this cellular population (Morest and Silver, 2003; Temple, 2001).

As noted in the introductory paragraphs, given the changing role of different glial cells at various stages of development and in the adult brain, it is not surprising that their numbers and density vary across the developmental time points that we measured as well as in different structures. Importantly, in adult *Monodelphis*, the number of glial cells far exceeds that of neurons. This observation is particularly important given the present understanding of glial cells in the adult CNS. Glial cells are no longer considered to be primarily supportive cells that passively maintain homeostatic conditions necessary for neurotransmission but rather actively participate in synaptic transmission. In recent years, a tripartite synapse, which contains pre- and postsynaptic neuronal elements as well as astrocytes that

encapsulate the synapse, has been described. Astrocytes have both ionotropic and metabotropic receptors that detect neurotransmitters, which increases internal stores of calcium within the astrocyte. This in turn causes gliotransmitters to be released at a slower rate than neurotransmitters and with a more prolonged affect. This bidirectional process is thought to modulate neurotransmission and plasticity (Pirttimaki and Parri, 2012; Santello et al., 2012; Verkhratsky et al., 2012). Given the importance of these cells in both homeostasis and active synaptic function, it is critical to appreciate the neuronal/glia cell relationships at a systems level. The relatively large proportion of glial cells in the adult *Monodelphis* suggests that their brains may rely heavily on glial cells (such as astrocytes) for assisting in the synaptic transmission of substantially fewer neurons. This supposition could be explored using the isotropic fractionator method following the generation of nuclear markers for different types of glial cells, such as microglia and astrocytes. Ultimately, these studies will lead to a greater understanding of how neuronal and glial populations interact and how those interactions may influence neural processing.

## ACKNOWLEDGMENTS

We thank Carol Oxford for her assistance at the UC Davis Flow Cytometry Shared Resource. We also thank Cindy Clayton, DVM, and the rest of the animal care staff at the UC Davis Psychology Department Vivarium.

## CONFLICT OF INTEREST STATEMENT

The authors have no conflicts of interest.

## ROLE OF AUTHORS

All authors had full access to all the data in the study and take responsibility for the integrity of the data and the accuracy of the data analysis. Study concept and design: AMHS, JCD, LAK. Acquisition of data: AMHS. Analysis and interpretation of data: AMHS. Drafting of the manuscript: AMHS, LAK. Critical revision of the manuscript for important intellectual content: AMHS, JCD, LAK. Statistical analysis: AMHS. Obtained funding: LAK. Administrative, technical, and material support: JCD. Study supervision: LAK.

## LITERATURE CITED

- Aitkin L, Nelson J, Farrington M, Swann S. 1991. Neurogenesis in the brain auditory pathway of a marsupial, the northern native cat (*Dasyurus hallucatus*). *J Comp Neurol* 309: 250–260.
- Anderson SA, Eisenstat DD, Shi L, Rubenstein JL. 1997. Inter-neuron migration from basal forebrain to neocortex: dependence on *Dlx* genes. *Science* 278:474–476.
- Bandeira F, Lent R, Herculano-Houzel S. 2009. Changing numbers of neuronal and nonneuronal cells underlie postnatal brain growth in the rat. *Proc Natl Acad Sci U S A* 106: 14108–14113.
- Baron G, Stephan H, Frahm HD. 1990. Comparison of brain structure volumes in Insectivora and primates. IX. Trigeminal complex. *J Hirnforschung* 31:193–200.
- Burish MJ, Peebles JK, Baldwin MK, Tavares L, Kaas JH, Herculano-Houzel S. 2010. Cellular scaling rules for primate spinal cords. *Brain Behav Evol* 76:45–59.
- Carletti B, Rossi F. 2008. Neurogenesis in the cerebellum. *Neuroscientist Rev J Neurobiol Neurol Psychiatry* 14: 91–100.
- Cheung AF, Kondo S, Abdel-Mannan O, Chodroff RA, Sirey TM, Bluy LE, Webber N, DeProto J, Karlen SJ, Krubitzer L, Stolp HB, Saunders NR, Molnar Z. 2010. The subventricular zone is the developmental milestone of a 6-layered neocortex: comparisons in metatherian and eutherian mammals. *Cereb Cortex* 20:1071–1081.
- Collins CE, Airey DC, Young NA, Leitch DB, Kaas JH. 2010a. Neuron densities vary across and within cortical areas in primates. *Proc Natl Acad Sci U S A* 107:15927–15932.
- Collins CE, Young NA, Flaherty DK, Airey DC, Kaas JH. 2010b. A rapid and reliable method of counting neurons and other cells in brain tissue: a comparison of flow cytometry and manual counting methods. *Front Neuroanat* 4:5.
- Cunningham CL, Martinez-Cerdeno V, Noctor SC. 2012. Microglia regulate neurogenesis in the developing cerebral cortex. *J Neurosci* (in press).
- Dehay C, Kennedy H. 2007. Cell-cycle control and cortical development. *Nat Rev Neurosci* 8:438–450.
- Finlay BL, Darlington RB. 1995. Linked regularities in the development and evolution of mammalian brains. *Science* 268:1578–1584.
- Frahm HD, Stephan H, Stephan M. 1982. Comparison of brain structure volumes in Insectivora and Primates. I. Neocortex. *J Hirnforschung* 23:375–389.
- Goldowitz D, Hamre K. 1998. The cells and molecules that make a cerebellum. *Trends Neurosci* 21:375–382.
- Herculano-Houzel S, Lent R. 2005. Isotropic fractionator: a simple, rapid method for the quantification of total cell and neuron numbers in the brain. *J Neurosci* 25: 2518–2521.
- Herculano-Houzel S, Mota B, Lent R. 2006. Cellular scaling rules for rodent brains. *Proc Natl Acad Sci U S A* 103: 12138–12143.
- Inta D, Alfonso J, von Engelhardt J, Kreuzberg MM, Meyer AH, van Hooft JA, Monyer H. 2008. Neurogenesis and widespread forebrain migration of distinct GABAergic neurons from the postnatal subventricular zone. *Proc Natl Acad Sci U S A* 105:20994–20999.
- Kriegstein AR, Noctor SC. 2004. Patterns of neuronal migration in the embryonic cortex. *Trends Neurosci* 27:392–399.
- Kumar SS, Buckmaster PS. 2007. Neuron-specific nuclear antigen NeuN is not detectable in gerbil substantia nigra pars reticulata. *Brain Res* 1142:54–60.
- Lyck L, Kroigard T, Finsen B. 2007. Unbiased cell quantification reveals a continued increase in the number of neocortical neurones during early post-natal development in mice. *Eur J Neurosci* 26:1749–1764.
- Marotte LR, Sheng X. 2000. Neurogenesis and identification of developing layers in the visual cortex of the wallaby (*Macropus eugenii*). *J Comp Neurol* 416:131–142.
- Martinez-Cerdeno V, Cunningham CL, Camacho J, Antczak JL, Prakash AN, Cziep ME, Walker AI, Noctor SC. 2012. Comparative analysis of the subventricular zone in rat, ferret and macaque: evidence for an outer subventricular zone in rodents. *PLoS one* 7:e30178.

- Miller FD, Gauthier AS. 2007. Timing is everything: making neurons vs. glia in the developing cortex. *Neuron* 54:357–369.
- Molnar Z, Knott GW, Blakemore C, Saunders NR. 1998. Development of thalamocortical projections in the South American gray short-tailed opossum (*Monodelphis domestica*). *J Comp Neurol* 398:491–514.
- Molyneaux BJ, Arlotta P, Hirata T, Hibi M, Macklis JD. 2005. Fezl is required for the birth and specification of corticospinal motor neurons. *Neuron* 47:817–831.
- Morest DK, Silver J. 2003. Precursors of neurons, neuroglia, and ependymal cells in the CNS: What are they? Where are they from? How do they get where they are going? *Glia* 43:6–18.
- Mouton PR. 2002. Principles and practices of unbiased stereology: an introduction for bioscientists. Baltimore: Johns Hopkins University Press.
- Mullen RJ, Buck CR, Smith AM. 1992. NeuN, a neuronal specific nuclear protein in vertebrates. *Development* 116:201–211.
- Nadarajah B, Parnavelas JG. 2002. Modes of neuronal migration in the developing cerebral cortex. *Nat Rev Neurosci* 3:423–432.
- Noctor SC, Martinez-Cerdeno V, Ivic L, Kriegstein AR. 2004. Cortical neurons arise in symmetric and asymmetric division zones and migrate through specific phases. *Nat Neurosci* 7:136–144.
- Noctor SC, Martinez-Cerdeno V, Kriegstein AR. 2008. Distinct behaviors of neural stem and progenitor cells underlie cortical neurogenesis. *J Comp Neurol* 508:28–44.
- Ooman S, Finckbone V, Dertien J, Attridge J, Henne W, Medina M, Mansouri B, Singh H, Strahlendorf H, Strahlendorf J. 2004. Active caspase-3 expression during postnatal development of rat cerebellum is not systematically or consistently associated with apoptosis. *J Comp Neurol* 476:154–173.
- Pirttimaki TM, Parri HR. 2012. Glutamatergic input-output properties of thalamic astrocytes. *Neuroscience* 205:18–28.
- Polazzi E, Contestabile A. 2002. Reciprocal interactions between microglia and neurons: from survival to neuropathology. *Rev Neurosci* 13:221–242.
- Puzzolo E, Mallamaci A. 2010. Cortico-cerebral histogenesis in the opossum *Monodelphis domestica*: generation of a hexalaminar neocortex in the absence of a basal proliferative compartment. *Neural Dev* 5:8.
- Rakic P. 1990. Principles of neural cell migration. *Experientia* 46:882–891.
- Robinson SR, Dreher B. 1990. The visual pathways of eutherian mammals and marsupials develop according to a common timetable. *Brain Behav Evol* 36:177–195.
- Sanchez-Villagra MR, Sultan F. 2002. The cerebellum at birth in therian mammals, with special reference to rodents. *Brain Behav Evol* 59:101–113.
- Sanderson KJ, Weller WL. 1990. Gradients of neurogenesis in possum neocortex. *Brain Res Dev Brain Res* 55:269–274.
- Santello M, Cali C, Bezzi P. 2012. Gliotransmission and the tripartite synapse. In: Kreutz MR, Sala C, editors. *Synaptic plasticity: dynamics, development, and disease*. New York: Springer. p 307–331.
- Sarko DK, Catania KC, Leitch DB, Kaas JH, Herculano-Houzel S. 2009. Cellular scaling rules of insectivore brains. *Front Neuroanat* 3:8.
- Sarnat HB, Noehlin D, Born DE. 1998. Neuronal nuclear antigen (NeuN): a marker of neuronal maturation in early human fetal nervous system. *Brain Dev* 20:88–94.
- Saunders NR, Adam E, Reader M, Mollgard K. 1989. *Monodelphis domestica* (grey short-tailed opossum): an accessible model for studies of early neocortical development. *Anat Embryol* 180:227–236.
- Stephan H, Frahm H, Baron G. 1981. New and revised data on volumes of brain structures in insectivores and primates. *Fol Primatol* 35:1–29.
- Stevens CF. 2001. An evolutionary scaling law for the primate visual system and its basis in cortical function. *Nature* 411:193–195.
- Temple S. 2001. The development of neural stem cells. *Nature* 414:112–117.
- Uppender MB, Naegel JR. 1999. Activation of microglia during developmentally regulated cell death in the cerebral cortex. *Dev Neurosci* 21:491–505.
- Verkhatsky A, Rodriguez JJ, Parpura V. 2012. Neurotransmitters and integration in neuronal-astroglial networks. *Neurochem Res* (in press).
- Wetts R, Herrup K. 1983. Direct correlation between Purkinje and granule cell number in the cerebella of lurcher chimeras and wild-type mice. *Brain Res* 312:41–47.
- Weyer A, Schilling K. 2003. Developmental and cell type-specific expression of the neuronal marker NeuN in the murine cerebellum. *J Neurosci Res* 73:400–409.
- Wichterle H, Turnbull DH, Nery S, Fishell G, Alvarez-Buylla A. 2001. In utero fate mapping reveals distinct migratory pathways and fates of neurons born in the mammalian basal forebrain. *Development* 128:3759–3771.
- Yan XX, Najbauer J, Woo CC, Dashtipour K, Ribak CE, Leon M. 2001. Expression of active caspase-3 in mitotic and postmitotic cells of the rat forebrain. *J Comp Neurol* 433:4–22.